Observed effects of the May 2024 Gannon Storm on the New Zealand gas pipeline network – towards predicting the effects of an extreme storm

M. Ingham[1], T. Divett[1], C. J. Rodger[2] and M. Sigley[3]

[1]School of Chemical and Physical Sciences, Victoria University of Wellington, Wellington, New Zealand.

[2]Department of Physics, University of Otago, Dunedin, New Zealand.

[3]FirstGas Ltd., New Plymouth, New Zealand.

Corresponding author: Malcolm Ingham (malcolm.ingham@vuw.ac.nz)

Key Points:

- Cathodic protection monitoring data from 33 locations on the New Zealand gas pipeline network during the Gannon Storm are discussed.
- Major variations in pipe to soil potentials were observed at a number of sites taking the potential outside the desired protection range.
- Analysis of these variations suggests approaches to modeling the likely effect of extreme geomagnetic storms on the network.

Abstract

We present cathodic protection monitoring data from the New Zealand gas pipeline network during the Gannon Storm of May 2024. At some locations potentials between the pipe and a $Cu/CuSO_4$ reference cell and between an installed metal coupon and the reference cell both underwent large variations - changes which took the pipeline outside the desired potential range for cathodic protection. At these locations both potentials became positive for significant lengths of time, which, in the event of defects in the pipe coating, can lead to corrosion of the pipe. Highly negative pipe to reference cell potentials, which can lead to detachment of the coating from the pipe, were also observed. Pipe to reference cell potentials and coupon to reference cell potentials are both indicators of the level of cathodic protection. The observed relationship between them when the rectifier is turned off are seen to have a complex form. Whilst the relationship is linear over a reasonably wide range of pipe to reference cell potentials, coupon-off potentials at some sites approach an asymptotic limit at highly negative pipe potentials, but rise sharply and become scattered at larger, including positive, pipe potentials. At locations where pipe to reference cell potentials are not routinely monitored, measurements of the potential between the anode bed and the pipe may be used to assess the level of cathodic protection. Assessment of the effects of the Gannon Storm allow the development of methods of predicting the effect of extreme storms on the network, which we put forward here.

Plain Language Summary

Variations in Earth's magnetic field during geomagnetic storms induce electric currents (geomagnetically induced currents) in the ground which, in certain circumstances, may disrupt the cathodic protection systems used to protect buried gas pipelines from corrosion. In this study we report the response of the New Zealand gas pipeline network to the Gannon Storm of May 2024, the largest geomagnetic storm for approximately 20 years. Studying and understanding the response of the pipeline network to this storm is important in developing methods to predict the likely response to extreme geomagnetic storms which may be up to 10 times larger and may present a risk to the integrity of the network.

1 Introduction

Geomagnetically induced currents present a potential risk to the cathodic protection (CP) systems (Gummow, 2002) that protect long pipelines from corrosion. Since the Effects on the Alaska pipeline were first recognized and investigated by Gideon (1971) and Campbell (1978, 1980), further studies have been conducted on pipelines in Argentina (Osella et al., 1998), Australia (Marshall et al., 2010, 2013), Canada (Fernberg et al., 2007), and Finland (Hajra, 2022; Pirjola et al., 2003; Pulkkinen et al., 2001; Viljanen, 1989; Viljanen et al., 2006, 2010). Studies have also been undertaken in New Zealand, as detailed below.

The effects of geomagnetically induced currents (GIC) on the New Zealand gas pipeline network have previously been discussed by Ingham et al. (2022) and Divett et al. (2023). Ingham et al. (2022) presented examples of monitoring data from 10 locations on the network and discussed the possible implications of GIC for the cathodic protection (CP) system that protects the pipeline. Divett et al. (2023) subsequently presented first attempts at modeling pipe to soil potentials on the New Zealand pipeline. Although the results of both studies were illuminating in showing the response of the pipeline network to geomagnetic activity, the magnetic storms used in the studies (Ingham et al. 2022, Table 1) were from the declining phase of Solar Cycle 24 and were of relatively small size, with only one storm reaching a Kp max of 7+. In contrast, the magnetic storm of 10-13 May 2024, the Gannon Storm, had a Kp max of 9- to 9 and the response of the pipeline network to this significantly larger storm may provide a more reliable guide to the potential impact of an extreme storm on the CP system.

In this paper we therefore present and discuss the observed effects of the Gannon Storm of May 2024 on the New Zealand pipeline network based on monitoring data from 33 locations across the network. We start with a review of the pipeline network, its CP system, and the parameters which are monitored. We then look, in turn, at specific aspects of the observed response of the pipeline to the storm and discuss approaches to predicting the likely effect of extreme geomagnetic activity on the network. Our industry partners are interested in the possible impact of extreme geomagnetic disturbances such as the Carrington event of 1859 (Carrington, 1859; Tsurutani, 2003), so they can quantify the risk to their infrastructure and systems. Such impacts extend from damage to aspects of the physical infrastructure to the possibility of enhanced corrosion at any defect in the pipe coating. Although we deal with the New Zealand pipeline network it is hoped that many of the conclusions will be relevant to pipeline networks in other countries.

2 The New Zealand gas pipeline network and CP system

The New Zealand gas pipeline network and the monitoring sites used in this paper are shown in Figure 1. As discussed by Ingham et al. (2022), and shown schematically in Figure 2, the CP system consists of a constant current rectifier at each of the sites, which applies a potential difference between an anode bed and the pipe such that the pipe is negative with respect to the adjacent ground. Both the rectifier output current and what Ingham et al. (2022) referred to as the “rectifier output voltage” are measured at each site with 1 s time resolution.

Also monitored at 1 second sampling at some rectifier sites are two other quantities. One of these is the potential difference between the pipe and a $Cu/CuSO_4$ reference cell near to the pipe. In the current study we refer to this potential difference as the pipe to soil potential (PSP). At a futher reduced number of sites a metal coupon is installed adjacent to the pipe and the potential difference between this and the reference cell (the coupon potential) is monitored. As explained by Gummow (2002) the pipe to reference cell potential is made up of two parts – the polarization potential between the pipe and the adjacent ground due to electrochemical effects, and the potential drop through the ground between the pipe and the reference electrode. This latter part is itself made up of two factors – the potential drop through the ground due to the cathodic protection current supplied by the rectifier and a time varying component resulting from the presence of GIC. This may be represented as

$$PSP = V_P + IR \pm V_{GIC} \quad (1)$$

where V_P is the polarization potential between the pipe and the adjacent ground, IR is the potential drop through the ground due to the cathodic protection current, and V_{GIC} is the contribution to the *PSP* due to geomagnetically induced current. When the rectifier is turned off the second term on the right-hand side of equation (1) is removed and the *PSP*, within the limits of any V_{GIC}, gives an estimate of the polarization potential. Here, we refer to the pipe to soil potential when the rectifier is turned on as *PSP-on*, and that when the rectifier is turned off as *PSP-off*.

To obtain an estimate of the polarization potential that does not include the effect of V_{GIC}, a metal coupon is installed close to the pipe surface. This simulates a defect in the pipeline coating. As explained by Gummow (2002), and shown in Figure 1 of Ingham et al. (2022) , it is connected to the pipe through a test station and the reference electrode is installed close to the coupon. Thus, when the rectifier is turned off the effects of both the cathodic protection current and GIC in equation (1) are removed, and the potential difference between the coupon and the reference electrode gives a measure of the polarization potential between the pipe and the ground. It is this potential difference between the coupon and the reference cell when the rectifier is turned off, referred to here as the “coupon-off” potential, which is regarded as the best measure of the polarization potential. The accepted industry standard is that the coupon-off potential should be in the range -0.85 V to -1.2 V to ensure that the pipe is protected (Popov & Lee, 2018). Polarization potentials higher than -0.85 V may expose the pipe to enhanced corrosion, while potentials significantly lower than -1.2 V may result in “disbonding” where the pipe coating becomes detached from the pipe (Ingham et al., 2022). Ackland & Dylejko (2019) discussed in detail the electrochemical reactions that take place at a pipe surface and how accurate a measure of the true polarization potential the coupon-off potential actually is. They concluded that the coupon-off potential (the “instant off potential” in their terminology) is always slightly more positive than the true polarization potential and represents the corrosion potential at the time of rectifier turn off – essentially a measure of the propensity of the pipe to oxidise in the environment to which it is exposed.

On the New Zealand pipeline network the interval between times when the rectifier is turned off varies from rectifier to rectifier, being only 5 or 10 minutes at some locations but up to 6 hours at others. At each turn off the rectifier is off for 3 seconds. The rectifiers on the New Zealand gas pipelines are normally set to give a constant current output, that is, the rectifier varies the output voltage to keep the protection current at a constant level, within set limits of the rectifier. As has been previously observed (Ingham et al., 2022) in general the current changes only slightly and this typically happens when there are rapid variations in the Earth's magnetic field, i.e., during significant space weather events. The rectifier voltage itself has a restricted range and the monitored "rectifier output voltage", like the pipe to reference cell potential, contains a time varying component due to GIC. It can therefore be more correctly identified as the total potential difference between the anode bed, through which the protection current is injected (Figure 2), and the pipe. It is the summation of the actual rectifier output voltage and the potential due to GIC passing onto and off the pipe. We subsequently refer to this as the anode bed to pipe potential (APP). The rectifier output voltage is controlled by pulse width modulation on a 38 Hz cycle, with the voltage set to achieve the necessary constant-current that keeps the pipe sufficiently negative with respect to ground with a 75% on pulse width modulation. Thus, an induced potential due to GIC of ~1.3x the 'normal' output voltage, will match the rectifier supply voltage and will drop the output current to zero, or in some instances possibly even reverse it. In this paper we draw distinction between the limited rectifier output voltage and the effect of GIC on APP.

3 The geomagnetic storm of 10-13 May 2024

The geomagnetic storm of 10-13 May 2024 was the largest event since at least the Halloween Storm of 2003, with a Kp index between 8- and 9 and these disturbance levels were sustained for a full 33 hours. As such it provides an excellent opportunity to investigate the impact that major geomagnetic activity has on the cathodic protection (CP) system on the New Zealand gas pipeline network. The magnetic field variations in the 1-second sampled northward (B_x) and eastward (B_y) components of the magnetic field as recorded over 10-13 May 2024 at the Eyrewell geomagnetic observatory, near Christchurch in New Zealand's South Island, are shown in Figure 3. Also shown in Figure 3 are the rates of change (in nT/min) of the two components. The storm commenced with a small increase in B_x at 1705 on 10 May with major variations of 100's of nT in both components occurring through until 0534 UT on 12 May. There was then a further burst of reduced activity starting at approximately 2100 UT on 12 May.

The maximum rates of increase of B_x and B_y were 360 and 192 nT/min respectively. The former occurred at 0846 UT on 11 May and was followed about 3 minutes later by the maximum rate of decrease of -191 nT/min. The maximum rate of increase in B_y occurred another 2 minutes later at 0851 UT, and was followed by a maximum rate of decrease in B_y of -164 nT/min some 5 minutes after this. These features are clearly seen as the prominent upward and downward spikes in the dB/dt panels in Figure 3. In comparison the maximum rates of change in B_x and B_y at Eyrewell during the largest storm studied by Ingham et al. (2022) were at least a factor of 10 smaller. As the Eyrewell observatory is approximately 300 km south of Wellington and 750 km south of Auckland it is likely, as was observed for the storm of 17 March 2015, discussed by Divett et al. (2020), that both the magnitude and rate of change of magnetic field across the pipeline network on 10-13 May 2024 were smaller than these observed values at Eyrewell. Nevertheless the Gannon storm represents the most significant observed geomagnetic activity in recent years, and, as stated above, gives the opportunity to assess both the impact of major activity on the pipeline network, and to allow progress to predicting the possible effects of an "extreme" storm.

4 Pipe to reference cell potential variations during the Gannon Storm

Pipe to soil potential (*PSP*) during geomagnetic activity can be calculated theoretically using the the equivalent-pi transmission line representation of a pipeline network as shown by Boteler (2013). This method has been used for preliminary calculations for the New Zealand pipeline network by Divett et al. (2023). It is pertinent therefore to review how the *PSP* at monitoring sites behaved during the Gannon Storm. This will go some way to giving insight into the likely "extreme" storm response. As reported by Ingham & Rodger (2018) on an earlier investigation at a single location in the New Zealand pipe network, when variations due to GIC cause the *PSP* to become positive, in the event of a defect in the pipeline coating, a corrosive current can pass from the pipe to the ground. Gummow (2002) summarized corrosion theory and calculated that, for a 1 cm^2 circular hole in a 0.3 mm thick modern pipeline coating, if the surrounding soil has a resistivity of 1000 Ωm the resulting current density due to a potential change of 1 V would be 2.5 mA/cm^2. This was calculated by the authors to give a corrosion rate of about 31.3 mm/year for a direct current. Allowing for a change in potential of ΔV, the dependence of corrosion rate on the period of the variation in potential, and the fraction of time (*t*) in a year that the change exists, the overall corrosion rate (*R*) in mm/year was expressed as

$$R = 31.3\, \Delta V \;\; t \;\; f \qquad (2)$$

where the factor *f* expresses the percentage effect of an alternating current compared to a direct current. It depends upon the period of the variation (*T*) in hours and, based on Figure 2 of Gummow (2002), may be expressed as

$$\log_{10} f \approx 0.18(\log_{10} T + 8.1) \qquad (3)$$

The authors thus calculated that a 0.5 V shift in potential could cause between 0.06 and 0.152 mm of corrosion per year depending on the period of the variation.

During the Gannon storm *PSP* were measured every second at 16 of the locations shown in Figure 1. Shown in Figure 4 are measured *PSP* at Salle Road (SR) over the 96 hours from 0000 UT on 10 May 2024 . It is apparent from Figure 4 that there were large variations in the measured *PSP* and values actually became positive for a substantial amount of the time. As outlined above, however, it is the *PSP* when the rectifier is turned off that is of most interest in assessing CP, and also the quantity which most closely aligns with *PSP* calculated using numerical modelling. Although measurements with the rectifier turned off are much less frequent than the 1 second basic sampling interval, if the *PSP* at each turn-off (*PSP-off*) is plotted against the potential immediately before turn-off (*PSP-on*) there is observed to be a very close relationship between the two quantities. It is observed that at all of the monitoring sites this relationship can be expressed as quadratic, as shown for example in Figure 5 for measurements at Salle Road. Applying this relationship to all the measured *PSP* at Salle Road allows the rectifier off *PSP* (*PSP-off*) to be calculated at the 1 second sampling rate.

Listed in Table 1, for the 48 hour period between 1200 UT 10 May 2024 to 1200 UT 12 May 2024, are the mean, maximum and minimum values of *PSP-off* at these 16 locations, calculated as described above, for the rectifier being turned off. Also listed is the cumulative lengths of time for which, at each location, *PSP-off* was positive and also the length of time when this quantity was less than -2 V. The variations in *PSP-off* over this time period for 8 of the sites where values were positive or less than -2 V for significant periods of time are shown in Figure 6. Maximum and minimum values that exceeded these values are shown in red in Table 1, and these limits are marked by the horizontal dashed lines in Figure 6.

As can be seen from Table 1 and Figure 6 the largest variations in *PSP-off*, with a range of over 12 V, occurred at Salle Road (SR), Waipu Cove Road (WCR) and Raukawa Road (RR). Salle Road and Waipu Cove Road are both at the northern end of the pipeline section which runs from Auckland to Whangarei (Figure 1), while Raukawa Road is towards the northeastern end of the line that runs to Hawkes Bay. These are the same three sites identified by Ingham et al. (2022) as being most susceptible to the effects of GIC. At these sites the *PSP-off* was positive for a significant part of the 48 hour period – nearly 20% of the time. There were also significant periods of positive *PSP-off* at Amriens Road (AR), Queen Elizabeth Park (QEP) and Waimana

	1200 UT 10 May 2024 – 1200 UT 12 May 2024				
Site	**Mean *PSP-off* (V)**	**Max *PSP-off* (V)**	**Min *PSP-off* (V)**	**t > 0 V (h:m:s)**	**t < -2 V (h:m:s)**
SR	-1.162	4.812	-11.400	8:48:03	7:22:02
WCR	-0.903	8.104	-13.813	8:35:25	7:12:39
KHR	-0.910	-0.011	-1.654	-	-
AR	-1.032	3.663	-4.268	2:12:37	3:37:43
MOH	-0.966	-0.100	-1.785	-	-
PR	-0.937	-0.242	-2.287	-	0:02:04
DR	-0.841	-0.625	-1.209	-	-
TPY	-0.616	-0.558	-0.78	-	-
QEP	-0.907	2.859	-4.766	3:14:59	3:10:38
TakR	-1.021	1.517	-4.890	1:44:59	1:26:23
JHR	-0.946	-0.397	-2.103	-	0:00:14
TB	0.306	3.038	-3.633	41:28:14	0:07:12
WaR	-1.230	4.472	-8.423	3:47:09	8:00:22
WhR	-1.169	0.017	-2.541	0:00:02	0:11:14
WtR	-0.735	0.577	-2.190	1:02:08	0:01:00
RR	-1.107	3.058	-9.039	8:29:22	7:45:34

Table 1: Mean, maximum and minimum values of pipe to reference cell potential calculated from the measured data for the when the rectifier is turned off. The period covered is from 1200 UT 10 May 2024 to 1200 UT 12 May 2024. Also listed are the cumulative lengths of time for which the calculated potential was positive and the cumulative lengths of time for which it was less than -2 V. Extreme values of *PSP* are marked in red.

Road (WaR). Of all the sites listed in Table 1, Tumunui Block (TB) stands out as having a mean value of *PSP-off* which is positive. This is vastly different from any other site and is highly anomalous. Although it is a situation which would normally indicate a high likelihood of corrosion, it has existed at Tumunui Block more or less since the rectifier was first installed nearly 50 years ago and no corrosion has been detected. This anomalous situation probably results from the locally complex volcanic and geothermal geology of an area which is also laced with a multitude of south-west to north-east trending faults.

The principal times at which the potential became positive at Salle Road, Waipu Cove Road and Raukawa Road were during the initial phase of the storm, and the periods for which the potential was continuously positive were several hours long. However, this was not the case at Amriens Road, Queen Elizabeth Park and Waimana Road. At these locations *PSP* became positive at different times and for much shorter periods. This difference results from the fact that the phase of GIC induced variations depends upon where on a segment of pipeline a site is located (Boteler and Seager, 1998; Ingham et al., 2022; Divett et al., 2023). Thus, at Salle Road and Waipu Cove Road, at the northern end of the section of pipeline from Auckland to Whangarei, rises in *PSP* were simultaneous with decreases in *PSP* at Amriens Road, which is at the southern end of this section of pipeline. Similarly, rises in potential at Queen Elizabeth Park were coincident with decreases in potential at Takapu Road (TakR) even though both locations are close to the southern end of the pipeline from Taranaki to Wellington. Thus, at Amriens Road, Queen Elizabeth Park and Waimana Road the instances of increased *PSP* were simultaneous with decreases at Salle Road, Waipu Cove Road and Raukawa Road, and typically were of much shorter duration.

As indicated by Ingham et al. (2022), and discussed in detail by Heim & Schwenk (1997), apart from the issue of corrosion resulting from positive potentials, extremely negative potentials carry the risk of the pipe coating becoming detached from the pipe, so called disbonding. Also shown in Table 1 are the lengths of time for which, at each site, the *PSP* was lower than -2 V. Although the value of -2 V is somewhat arbitrary, it is apparent that almost all the same sites which show positive *PSP-off* potentials are those that show highly negative values. Thus, sites susceptible to large variations in *PSP* are potentially at risk both of corrosion and of disbonding. Potentials less than -2 V also occurred at Salle Road, Waipu Cove Road and Raukawa Road for significant lengths of time, although the longest length of time for which potentials were less than -2 V was at Waimana Road. As for the positive *PSP-off* potentials at Salle Road, Waipu Cove Road and Raukawa Road, this was during the initial phase of the storm and resulted in long periods of the potential being continuously lower than -2 V. Significant periods of very negative potentials also occurred at Amriens Road, Queen Elizabeth Park and Takapu Road.

Equation (2) suggests the possibility of a rough calculation of the effective corrosion rate due to the Gannon Storm. Although the maximum values of potential listed in Table 1 were significantly higher, the average value of positive potential at Salle Road and Raukawa Road were slightly less than 1 V, with the corresponding value at Waipu Cove Road being about 1.5 V – rises in potential from the mean values of about 2.5 V. Also relevant is the typical period *T* of the variation in potential which gives rise to positive values. At these three locations, as noted above, the dominant period of this variation, at least in the early part of the Gannon Storm, is about 3 hours. Thus, taking $\Delta V \approx 2.5$ V, a value of f of approximately 0.35 (expressed as a percentage, calculated from the period of 3 hours using equation (3)), and taking the 48 hours of the storm shown in Figure 6 as 0.0055 of a year, leads to a calculated corrosion rate of 0.151 mm/year. This represents a first order estimate of the rate calculated from the effect of a single storm of K_P between 8 and 9 and is close to the maximum value quoted by Gummow (2002) for the cumulative effect of multiple smaller storms.

5 Coupon-off potential variations during the Gannon Storm

Notwithstanding the discussion of the variations in *PSP* when the rectifier is turned off, as indicated previously, the industry standard for deeming if a pipe is protected comes from the potential between an installed coupon and a $Cu/CuSO_4$ reference cell, also when the rectifier is turned off. Shown in Figure 7 are *coupon-off* measurements from 6 sites during the most intense period of geomagnetic activity from 1200 UT 10 May 2024 to 1200 UT 12 May 2024. Measurements at Salle Road, Waipu Cove Road and Amriens Road were made every 5 minutes, whilst at the other three sites the interval between measurements was 10 minutes. Also shown are the -0.85 V and -1.2 V limits that it is recommended that the potential should be between. Table 2 lists the mean, maximum and minimum values of the *coupon-off* potentials at all sites where it was measured for the 96 hours from 0000 10 May 2024 to 0000 14 May 2024 UT.

As can be seen from Figure 7, rises in *coupon-off* potential above the recommended upper limit of -0.85 V occurred at all of the sites shown. At Waipu Cove Road, Queen Elizabeth Park and Waimana Road the *coupon-off* potential actually became positive at times. As for *PSP-off*, the timing of such instances was not coincident at each site. This is best evidenced by the differences between Waipu Cove Road and Queen Elizabeth Park during the first part of the storm. At Waipu Cove Road the GIC induced by the initial decrease in B_x, seen in Figure 3, caused the *coupon-off* potential to rise above -0.85 V, while at Queen Elizabeth Park the potential actually became more negative. Again, as for the *PSP-off* this is related to the difference in phase of variations due to GIC depending on the location of the site.

Table 2 shows that the *coupon-off* potential also rose above -0.85 V at Komokoriki Hill Road (KHR), Mahoenui (MOH), Lower Duthie Road (DR), Tempsky Road (TPY) and Tumunui Block (TB), although, apart from at Lower Duthie Road, the mean level of the potential was above or very close to this value. At Lower Duthie Road, where the sampling interval of *coupon-off* potential was 60 minutes, only a single measurement in the 96 hours shown exceeded this value. Similarly, the *coupon-off* potential became lower than -1.2 V at seven of the sites listed in Table 2. At Waipu Cove Road (WCR), Pembroke Road (PR), Takapu Road (TakR) and Whatatutu Road (WhR) the mean level of the potential was slightly lower than this value. The most extreme negative potentials by far were seen at Waipu Cove Road and Queen Elizabeth Park (QEP). At the latter site the range of variation was such that almost 30% of the *coupon-off* potentials measured over 96 hours were outside the desired range of -0.85 to -1.2 V. The vast majority of these were during the 48 hour period from 1200 UT 10 May 2024 to 1200 UT 12 May 2024.

Coupon-off potentials were not measured at Raukawa Road where, as seen in Table 1 and Figure 5, there were large variations in values of *PSP* when the rectifier was turned off. As might be expected, and as is discussed below, there is a close correlation between variations in such pipe to reference cell measurements and *coupon-off* measurements. That being the case it can be inferred that large variations in the cathodic protection level, as given by *coupon-off* measurements, similar in magnitude to those seen at Waipu Cove Road, are also very likely to have occurred at Raukawa Road.

	0000 UT 10 May 2024 – 0000 UT 14 May 2024			
Site	**Mean coupon-off potential (V)**	**Max coupon-off potential (V)**	**Min coupon-off potential (V)**	**Sample interval (m)**
SR	-1.098	-0.107	-1.315	5
WCR	-1.426	0.526	-2.556	5
KHR	-0.853	-0.798	-0.916	5
AR	-1.130	-0.653	-1.167	5
MOH	-0.794	-0.742	-0.850	60
PR	-1.261	-1.247	-1.271	60
DR	-1.068	-0.508	-1.199	60
TPY	-0.763	-0.731	--0.786	60
QEP	-0.974	1.503	-2.429	10
TakR	-1.285	-0.683	-1.312	10
TB	0.026	0.127	-0.138	10
WaR	-1.174	0.563	-1.343	10
WhR	-1.294	-1.259	-1.337	10

Table 2: Mean, maximum and minimum values of coupon-off potentials for the period 0000 UT 10 May 2024 to 0000 UT 14 May 2024. Values shown in red are those outside the -0.85 to -1.2 V range.

Although both *coupon-off* and *PSP-off* potentials can be considered as indicators of the efficacy of cathodic protection on the pipeline, the relationship between them is not simple. At most sites where the *PSP-off* potential both reached highly negative values and become positive at times, such as Salle Road, Takapu Road and Waimana Road, there are three distinct features in the relationship between *coupon-off* and *PSP-off* potentials, as shown in Figure 8. At highly negative *PSP-off* potentials the *coupon-off* potential approaches a constant value. This asymptotic behavior has been discussed by Ackland & Dylejko (2019) and related to the electrochemical equilibrium between Fe in an aqueous environment and Fe_3O_4. At intermediate values of *PSP-off* the relationship between the two potentials is highly linear. This linearity breaks down at higher values of *PSP-off* when the corresponding values of *coupon-off* potential become very scattered, although at some sites (e.g., Waimana Road) there is an indication that there may also be a limiting upper value of *coupon-off* potential.

At other sites, such as Komokoriki Hill Road and Whatatutu Road, also shown in Figure 8, where the variations in *PSP-off* are not as extreme, only the linear portion of this relationship is apparent and there is no obvious indication of the asymptotic approach to a lower limit of *coupon-off* potential at highly negative *PSP-off*. Apart from Komokoriki Hill Road and Whatatutu Road, all of the monitored sites where only linearity is observed, are ones where the pipeline has the more conductive coal-tar coating. It is therefore tempting to attribute this difference in behavior to the nature of the coating, especially as at Queen Elizabeth Park (Figure 8), where the coating is coal-tar, linearity in the relationship persists to positive values of the *PSP-off* potential.

6 Anode bed to pipe potential variations during the Gannon Storm

Although the variations in *PSP-off* and *coupon-off* potentials give a guide to locations where the pipeline may be at risk as a result of major geomagnetic activity, the relatively small number of sites where *PSP* is monitored means that the coverage is somewhat limited. The potential between the anode bed and the pipe (*APP*), however, is monitored at every rectifier and gives the most widespread coverage of the effect of GIC on the network. *APP* can be regarded as the sum of a potential drop (IR) between the anode bed and the ground immediately adjacent to the pipe, essentially the rectifier current times the ground "resistance", and the potential drop between the ground outside the pipe and the pipe surface. This second term can effectively be regarded as the negative of the *PSP*, hence

$$APP = IR - PSP \qquad (4)$$

As is discussed further below, the rectifier current is constant except during major rapid changes in potential and the term IR may therefore, to a very good approximation, be considered as constant over the duration of a storm. This means that, if the mean value of *APP* is subtracted from *APP,* and the mean value of *PSP* is subtracted from *PSP*, the resulting potentials (APP_0 and PSP_0) are related by

$$APP_0 = -PSP_0 \qquad (5)$$

The anode to pipe potential variations treated in this manner can be seen as a guide to how *PSP* varies at sites where it is not monitored. This relationship is illustrated in Figure 9 which shows, for Salle Road, both the measured PSP_0 and $-APP_0$. The correlation coefficient between the two series is 0.992. Also shown are plots of PSP_0 and $-APP_0$ when the rectifier was turned off. The similarity between these suggests that at sites where pipe to reference cell potentials are not measured, the anode to pipe potentials when the rectifier is turned off can be used as a suitable proxy for assessing the behavior of the cathodic protection system at that site.

Measured anode bed to pipe potentials from four locations are shown in Figure 10. The absolute range of the variations in *APP* differs from site to site, the largest, approximately 7 V, being at Waitao Road which is on the coast in the Bay of Plenty (Figure 1). At this site the *APP* actually became negative for a short period of time at just after 0730 UT on 11 May 2024. At the other three sites the range of the variations is between 1.5 and 4.5 V. Apparent from Figure 10, as is the case for *PSP*, is a 180° phase difference between variations at Timaru Road and Te Horo Beach Road when compared to Waitao Road and Shewan Road. Also noticeable is a difference between the average *APP* at the four sites. This is significantly higher at Timaru Road and Te Horo Beach Road (> 10 V) than at either Waitao Road or Shewan Road (< 5 V). This difference in the average level of *APP* is related to the different pipeline coatings, and is significantly higher on those sections of pipeline (principally from Taranaki north to Auckland and south to Wellington) which are coated with coal-tar compared to those coated with more modern and less conductive coatings. It results from the necessity for a higher rectifier output voltage being required to supply the necessary current and negative potential to the pipe on coal-tar coated sections.

7 Rectifier current "collapse"

As detailed above the rectifiers supplying the cathodic protection to the New Zealand pipeline network are set to provide a constant current. Thus, except in cases of rapid magnetic field variations there is little change in current (e.g. Figure 2, Ingham et al., 2022). During the Gannon Storm, however, at some locations there were major variations in rectifier output current. These included not only significant increases in current but also some instances where the current dropped to zero. Such occurrences were at sites where major variations in the observed pipe to reference cell potential occurred. An example, from Waipu Cove Road, is shown in Figure 11.

This behavior can be understood by recalling that, just as the measured pipe to reference cell potential is made up of separate parts, as expressed in equation (1), the anode to pipe potential (*APP*) is made up of two parts – the potential difference supplied by the actual rectifier, and a potential due to GIC. The left hand panels of Figure 12 show an expanded time section of the variations in rectifier current output and pipe to reference cell potential at Waipu Cove Road over a period of 5 hours. Four major instances where the output current effectively became zero are marked. It is apparent that these "collapses" of current supply occurred when the pipe to reference cell potential became more negative than a limit shown by the red horizontal dashed line. It can be inferred that at these times the effect of GIC on the pipe was to make it sufficiently negative that no current was required from the rectifier itself to supply the cathodic protection – in effect protection was being supplied by the GIC. In contrast, when the pipe to reference cell potential increased, including above zero, the rectifier current was either above or at its normal constant value. Inspection of the effect on the measured coupon-off potentials suggests that it is only during these rapid increases in *PSP* that there is a significant change, with *coupon-off* potentials, as evidenced in Figure 7 also rising, sometimes above the -0.85 V level. This relates to the fact that the actual output voltage of the rectifier is limited and cannot rise above a set maximum value.

The upper right-hand panel of Figure 12 shows the anode to pipe potential when the rectifier was turned off. This is essentially the contribution to the anode to pipe potential resulting from GIC. The instances of current collapse coincide with increases in *APP-off* above a certain level, again indicating that GIC are causing the pipe to be sufficiently negative that it is protected. If the *APP-off* potential represents the contribution of GIC to measured *APP*, then subtracting this from the measured *APP* immediately before rectifier turn-off gives an approximation to the actual output voltage of the rectifier. This is shown in the lower right-hand panel of Figure 12, and shows, within the limits of the 5-minute sampling at Waipu Cove Road, that the rectifier output voltage does indeed decline dramatically during the periods of current collapse.

8 Towards predicting extreme storm pipeline effects

It is apparent from the results presented above that during the Gannon Storm measurements of both *PSP-off* and *coupon-off* potential indicate that certain sites on the New Zealand pipeline network showed variations in these quantities which took the pipe outside the desired cathodic protection range. The estimated corrosion rate at these sites, due to rises in *PSP*, caused by this single *Kp* max 9- to 9 storm was about 0.15 mm/year. Despite the added knowledge gained from the Gannon Storm, the likelihood of disbonding due to large decreases in *PSP* still remains unquantified, although sites subject to risk due to rises in *PSP* are, largely, also those susceptible to significant decreases in *PSP*. An “extreme” storm is estimated to have magnetic field variations at least of the order of 10 times larger than the Gannon Storm for New Zealand latitudes (Hapgood et al., 2021; Mac Manus et al., 2022), which would lead to much larger variations in both *PSP-off* and *coupon-off* potentials and, presumably, increase the estimated rate of corrosion by a similar factor. Calculating the predicted possible effects of an extreme storm on the pipeline network is therefore of significant interest. There are two potential ways in which this may be done.

The first method, which would allow calculation of the likely effects everywhere on the pipeline network, is through numerical modeling using the methods of Boteler and Cookson (1986) or Boteler (2013) to calculate *PSP* resulting from synthetic extreme storms. As has been discussed above, the calculated variations in *PSP* can be related to the possibility of both corrosion (including numerical calculation as per Gummow (2002)) and disbondment. At sites where a relationships between *PSP* and *coupon* potentials can be formulated such calculations may also yield the likely variations in *coupon-off* potential.

A second potential approach is to use measured data from the monitoring sites on the New Zealand pipeline network in a manner akin to the following.

i. At each monitoring site where data are available, use measured *PSP-on* data during multiple past geomagnetic storms to calculate transfer functions between *PSP-on* and the magnetic field variations at Eyrewell geomagnetic observatory. This is effectively similar to the approach taken by Ingham et al. (2017) to estimate GIC in the New Zealand power network. Note that the use of transfer functions between observations and Eyrewell observations means that differences between the magnetic field at Eyrewell and across the North Island do not matter.

ii. For a synthetic extreme storm use the transfer functions to calculate the response of *PSP-on* to the storm. The type of relationship shown in Figure 5 between *PSP-off* and *PSP-on* can be used to transform this into the predicted response of *PSP-off*.

iii. As for the direct modelling method, observed relationships between *PSP* and coupon potentials may then, in principle, be used to calculated how *coupon-off* potentials vary.

iv. For locations where *PSP* are not measured a similar procedure can be used by calculating transfer functions between *APP* and the magnetic field. Relating *APP* when the rectifier is on to *APP-off*, and equation (3) can then be used to calculate the expected variations in *PSP-off*.

Ultimately, comparison of the results of these two approaches should give confidence in the predicted response of the network to an extreme storm. This should allow our industry partners to determine the hazard levels to their network infrastructure.

9 Summary

We have presented here observations and discussion of the effects of the Gannon Storm on the New Zealand pipeline network. The main observed features are as follows.

- Major variations in *APP*, *PSP*, and *coupon-off* potential occurred at several sites, taking the cathodic protection system outside its designated “safe” region. The sites most affected on the northern section of pipe from Auckland to Whangarei were Salle Road, Waipu Cove Road and Amriens Road. At the southern end of the pipeline network the largest variations were at Queen Elizabeth Park and Takapu Road, just to the north of Wellington. Very large variations were also seen at Raukawa Road in Hawkes Bay, and at Waimana Road in eastern Bay of Plenty. Possible corrosion rates due to the storm approached 0.15 mm/year. At several sites the average level of *coupon-off* potential was actually outside the -0.85 to -1.2 V limits, while highly anomalous potentials were observed at Tumunui Block.

- At many sites the relationship between *PSP-off* and *coupon-off* potentials shows that the *coupon-off* potential approaches an asymptotic limit at very negative values of *PSP-off*, but becomes scattered at high, positive, values of *PSP-off*. At other sites the relationship between these quantities is essentially linear. There is a suggestion this difference in the relationships, as well as that between mean levels of anode bed to pipe potential, may be related to the nature of the pipeline coating.

- At some sites where variations in *PSP* are large it is apparent that highly negative values of *PSP* resulting from GIC do themselves provide cathodic protection and the rectifier current output and voltage drop to close to zero. There is no apparent effect on *coupon-off* potentials.

- At rectifier sites where pipe to reference cell potentials are not monitored the measurements of *APP* reduced to zero mean are shown to be very nearly equal to the negative of *PSP* measurements, also reduced to zero mean.

Study of these effects of the Gannon Storm is aiding the development of methods and procedures for predicting the possible effects of an extreme storm on the New Zealand gas pipeline network. Future studies are planned to apply those methods and hence determine the importance of space weather extreme events to this important industry.

Acknowledgments

This research was supported by the New Zealand Ministry of Business, Innovation & Employment Endeavour Fund Research Programme Contract UOOX2002.

Data Availability Statement

Cathodic protection monitoring data reported here are the property of First Gas New Zealand Ltd. Request for access to the data should be addressed in the first instance to Mark Sigley (mark.sigley@firstgas.co.nz). Magnetic observatory data from Eyrewell may be downloaded from www.intermagnet.org.

References

Ackland, B. & Dylejko, K.P. (2019) . Critical questions and answers about cathodic protection. *Corrosion Engineering, Science and Technology*, 54(8), 688-697, doi:10.1080/1478422X.2019.1658437.

Boteler, D. H. (2013). A new versatile method for modelling geomagnetic induction in pipelines. *Geophysical Journal International*, *193*(1), 98-109, doi:org/10.1093/516gji/ggs113

Boteler, D. H. & M. Cookson (1986). Telluric currents and their effects on pipelines in the Cook Strait region of New Zealand. *Materials Performance*, 25(3), 27 – 32.

Boteler, D. & W.H. Seager (1998). Telluric currents: a meeting of theory and observation. *Corrosion*, 54(9), 751-755. https://doi.org/10.5006/1.3284894.

Campbell, W. H. (1978). Induction of auroral zone electric currents within the Alaskan pipeline. *Pure and Applied Geophysics*, *116*(6), 1143-1173. https://doi.org/10.1007/bf00874677.

Campbell, W. H. (1980). Observation of electric currents in the Alaskan oil pipeline resulting from auroral electrojet current sources. *Geophysical Journal of the Royal Astronomical Society*, *61*(2), 437 – 449. https://doi.org/10.1111/j.1365-246x.1980.tb04325.x.

Carrington, R. C. (1859). Description of a singular appearance seen in the Sun on September 1, 1859. *Monthly Notices of the Royal Astronomical Society*, 20, 13–15. https://doi.org/10.1093/mnras/20.1.13.

Divett, T., Mac Manus, D.H., Richardson, G.S., Beggan, C.D., Rodger, C.J., Ingham, M., Clarke, E., Thomson, A.W.P., Dalzell, M. & Obana, Y. (2020). Geomagnetically induced current model validation from New Zealand's South Island. *Space Weather*, 18, e2020SW002494. https://doi.org/10.1029/2020SW002494.

Divett, T., Ingham, M., Richardson, G., Sigley, M., & Rodger, C. J. (2023). Modeling pipe to soil potentials from geomagnetic storms in gas pipelines in New Zealand. *Space Weather*, *21*, e2023SW003601. https://doi.org/10.1029/2023SW003601.

Gideon, D. N. (1971). Telluric current effects on buried pipelines. *Materials Protection and Performance*, 5 – 10.

Gummow, R. A., 2002. GIC effects on pipeline corrosion and corrosion control systems. *Journal of Atmospheric and Solar-Terrestrial Physics*, *64*(16), 1755–1764. https://doi.org/10.1016/s1364-6826(02)00125-6.

Hajra, R. (2022). Intense, long-duration geomagnetically induced currents (GICs) caused by intense substorm clusters. *Space Weather*, *20*(3). https://doi.org/10.1029/2021SW002937.

Hapgood, M., Angling, M. J., Attrill, G., Bisi, M., Cannon, P. S., Dyer, C., et al. (2021). Development of space weather reasonable worst-case scenarios for the UK National Risk Assessment. *Space Weather*, 19(4), e2020SW002593. https://doi.org/10.1029/2020SW002593.

Heim, G. & Schwenk, W. (1997). Coatings for Corrosion Protection. In W. von Baeckmann, H. Bohnes, G. Franke, D. Funk, C. Gey, H. Gräfen, G. Heim, V. Heinzelmann, K. Horras, B. Isecke, H. Kampermann, B. Leutner, H. -U. Paul, F. Paulekat, W. Prinz, B. Richter, G. Rieger, H.G. Schöneich, W. Schwenk (Eds*), Handbook of Cathodic Corrosion Protection (Third Edition)*. https://doi.org/10.1016/B978-088415056-5/50012-5.

Ingham, M. & Rodger, C.J. (2018). Telluric field variations as drivers of variations in cathodic protection potential on a natural gas pipeline in New Zealand. *Space Weather*, 16, 1396-1409. https://doi.org/10.1029/2018SW001985.

Ingham, M., Rodger, C.J., Divett, T., Dalzell, M. & Petersen, T. (2017). Assessment of GIC based on transfer function analysis. I, 15, 1615-1627. https://doi.org/10.1002/2017SW001707.

Ingham, M., Divett, T., Rodger, C. J., & Sigley, M. (2022). Impacts of GIC on the New Zealand gas pipeline network. *Space Weather*, *20*, e2022SW003298. https://doi.org/10.1029/2022SW003298.

Mac Manus, D. H., Rodger, C. J., Dalzell, M., Renton, A., Richardson, G. S., Petersen, T., & Clilverd, M. A. (2022). Geomagnetically induced current modeling in New Zealand: Extreme storm analysis using multiple disturbance scenarios and industry provided hazard magnitudes. Space Weather, 20(12), e2022SW003320. https://doi.org/10.1029/2022SW003320.

Marshall, R. A., Waters, C. L., & Sciffer, D. (2010). Spectral analysis of pipe to soil potentials with variations of the Earth's magnetic field in the Australian region. *Space Weather*, *8*(5), S05002. https://doi.org/10.1029/2009SW000553.

Marshall, R. A., Gorniak, H., Van Der Walt, T., Waters, C. L., Sciffer, M. D., Miller, M., et al. (2013). Observations of geomagnetically induced currents in the Australian power network. *Space Weather*, *11*(1), 6 – 16. https://doi.org/10.1029/2012SW000849.

Osella, A., Favetto, A., & Lopez, E. (1998). Currents induced by geomagnetic storms on buried pipelines as a cause of corrosion. *Journal of Applied Geophysics*, *38*(3), 219 – 233. https://doi.org/10.1016/s0926-9851(97)00019-0.

Pirjola, R., Pulkkinen, A., & Viljanen, A. (2003). Studies of space weather effects on the Finnish natural gas pipeline and on the Finnish high-voltage power system. *Advances in Space Research*, *31*(4), 795 – 805. https://doi.org/10.1016/S0273-1177(02)00781-0.

Popov, B. N., & Lee, J.-W. (2018). Cathodic protection of pipelines. In M. Kurtz (Ed.), *Handbook of environmental degradation of materials* (pp. 509–532). https://doi.org/10.1016/B978-0-323-52472-8.00023-3.

Pulkkinen, A., Viljanen, A., Pajunp.., K., & Pirjola, A. (2001). Recordings and occurrence of geomagnetically induced currents in the Finnish natural gas pipeline network. *Journal of Applied Geophysics*, *48*(4), 219 – 231. https://doi.org/10.1016/s0926-9851(01)00108-2.

Tsurutani, B. T. (2003). The extreme magnetic storm of 1–2 September 1859. *Journal of Geophysical Research*, 108 (A7), 1268. https://doi.org/10.1029/2002JA009504.

Viljanen, A. (1989). Geomagnetically induced currents in the Finnish natural gas pipeline. *Geophysica*, *25*, 135 – 159.

Viljanen, A., Koistinen, A., Pajunp.., K., Pirjola, R., Posio, P., & Pulkkinen, A. (2010). Recordings of geomagnetically induced currents in the Finnish natural gas pipeline—Summary of an 11-year period. *Geophysica*, *46*(1 – 2), 59 – 67.

Viljanen, A., Pulkkinen, A., Pirjola, R., Pajunp.., K., Posio, P., & Koistinen, A. (2006). Recordings of geomagnetically induced currents and a nowcasting service of the Finnish natural gas pipeline system. *Space Weather*, *4*(10), S10004. https://doi.org/10.1029/2006SW000234.

Figure captions

Figure 1: The New Zealand gas pipeline network. Red lines—pipelines coated with coal-tar enamel; blue lines—pipelines with other, lower conductance, coatings; gray dots – earthing beds; red dots—rectifier locations, with those used in this study named: SR – Salle Road, WCR – Waipu Cove Road, KHR – Komokoriki Hill Road, AR – Amriens Road, ONH – Onehunga, AmP – Ambury Park, IR - Ingram Road, TUA – Tuakau, ROT - Rotowaro Road, SWR - Shewan Road, LBR - Lees Block Road, MOH – Mahoenui, TGP – Tongapurutu, TR - Timaru Road, PR - Pembroke Road, DR - Lower Duthie Road, TPY - Tempsky Road, TBR - Turakina Beach Road, PPR - Pukepuke Road, HBR - Hokio Beach Road, THBR -Te Horo Beach Road, QEP - Queen Elizabeth Park , GR - Grays Road, TakR - Takapu Road, WTO - Waitao Road, WHE - Whites Road, JHR - Jack Henry Road, TB - Tumunui Block, OR - Okaro Road, WaR - Waimana Road, WhR -Whatatutu Road, WtR - Watershed Road, RR - Raukawa Road.

Figure 2: Schematic diagram of a CP monitoring site. Monitored quantities are: (i) the potential between the anode bed and the pipe (*APP*), (ii) the current supplied by the rectifier, (iii) the potential between the pipe and the Cu/$CuSO_4$ reference electrode (*PSP*), (iv) the potential between the metal coupon and the reference electrode (*coupon*).

Figure 3: Left-hand panels show the variations in the northward (B_x) and eastward (B_y) components of the magnetic field recorded at Eyrewell geomagnetic observatory from 0000 UT 10 May 2024 until 0000 UT 13 May 2024. Shown in the right-hand panels are the rates of change of B_x and B_y in nT/min.

Figure 4: Measured pipe to reference cell potential at Salle Road during the period 0000 UT 10 May 2024 to 0000 UT 13 May 2024.

Figure 5: *PSP* at Salle Road when the rectifier is turned off (PSP-off) plotted against the potential immediately before turn-off (PSP-on). The red line shows the quadratic fit indicated.

Figure 6: Pipe to soil potentials with the rectifier turned off (*PSP-off*) calculated for 8 sites on the pipeline network during the period 1200 UT 10 May 2024 to 1200 UT 12 May 2024. The dashed lines mark 0 V and -2 V as discussed in the text.

Figure 7: Coupon-off potentials measured at 8 sites on the pipeline network during the period 1200 UT 10 May 2024 to 1200 UT 12 May 2024. Also shown by the dashed lines are the recommended -0.85 V and -1.2 V limits for safe cathodic protection.

Figure 8: Coupon-off potential plotted against PSP-off at 6 sites. The nature of the pipeline coating at each site is indicated: S – synthetic, CT – coal tar.

Figure 9: Measured values of the pipe to soil potential (PSP_0) and the negative of the anode bed to pipe potential (APP_0), both reduced to zero mean, at Salle Road for the period 0000 UT 10 May 2024 to 0000 UT 14 May 2024. The left-hand column shows measurements when the

rectifier was turned on. The right-hand column shows measurements when the rectifier was turned off.

Figure 10: Anode bed to pipe potential measured at 4 sites for the 48 hours from 1200 UT 10 May 2024 to 1200 UT 12 May 2024.

Figure 11: Variations in rectifier output current at Waipu Cove Road.

Figure 12: Variations in rectifier output current, pipe to reference cell potential, *APP-off* potential and calculated rectifier output over a 5 hour period at Waipu Cove Road.

Figure 1.

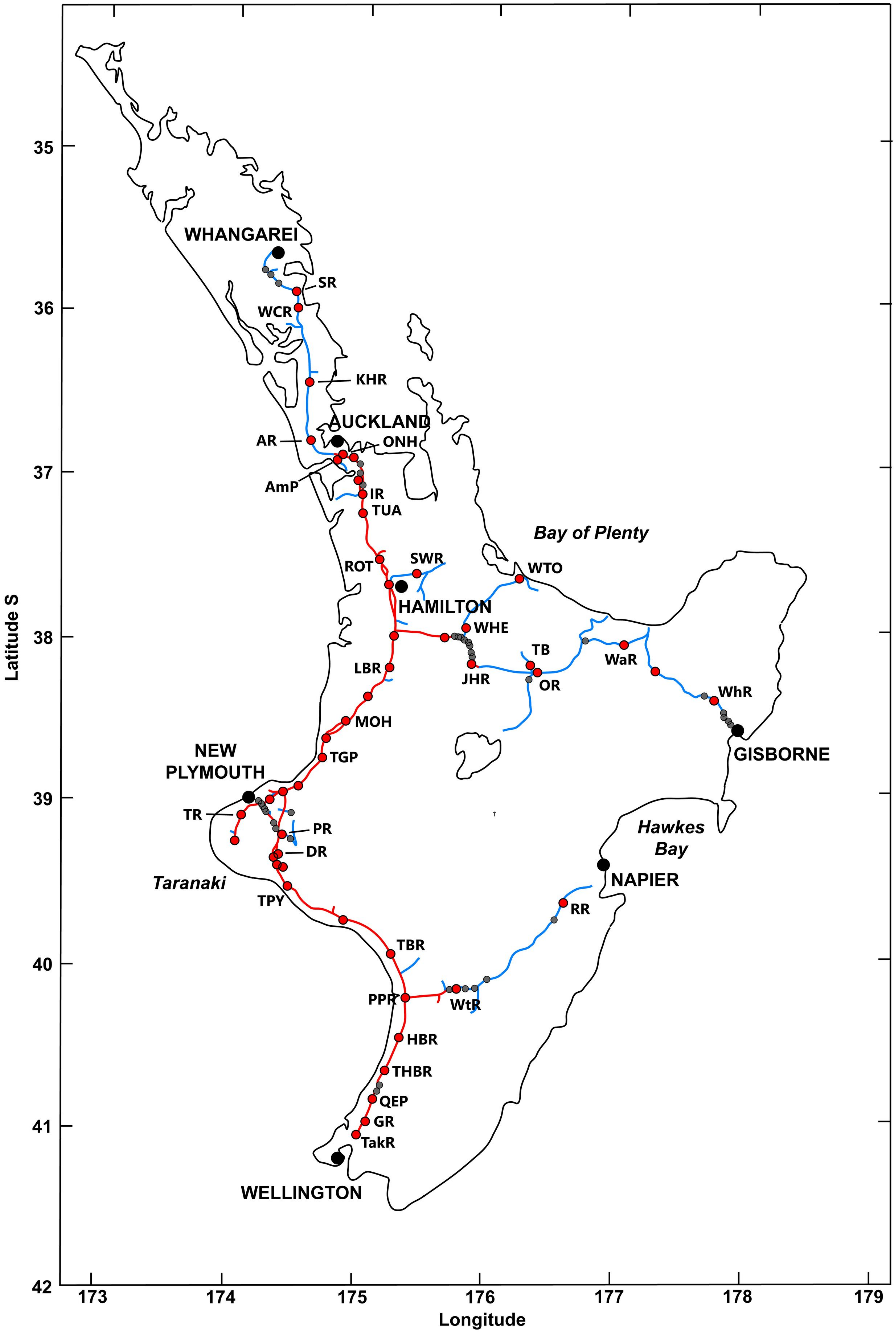

WHANGAREI
SR
WCR
KHR
AUCKLAND
AR
ONH
AmP
IR
TUA
Bay of Plenty
ROT
SWR
WTO
HAMILTON
WHE
TB
LBR
JHR
OR
WaR
WhR
MOH
GISBORNE
NEW PLYMOUTH
TGP
TR
PR
DR
Hawkes Bay
Taranaki
NAPIER
TPY
RR
TBR
PPR
WtR
HBR
THBR
QEP
GR
TakR
WELLINGTON
Latitude S
Longitude
35
36
37
38
39
40
41
42
173
174
175
176
177
178
179

Figure 2.

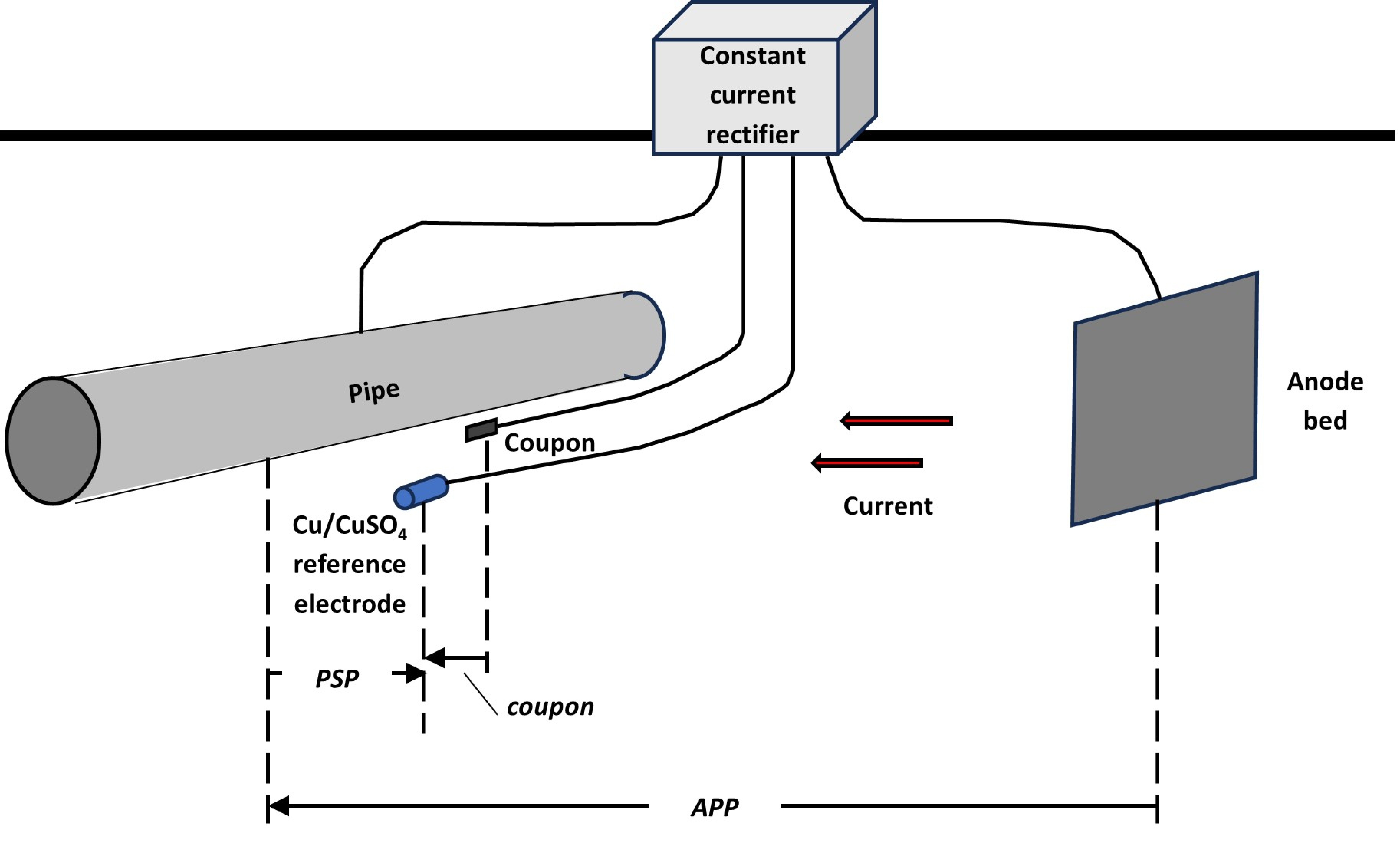
Constant current rectifier
Pipe
Coupon
Cu/CuSO4 reference electrode
Current
Anode bed
PSP
coupon
APP

Figure 3.

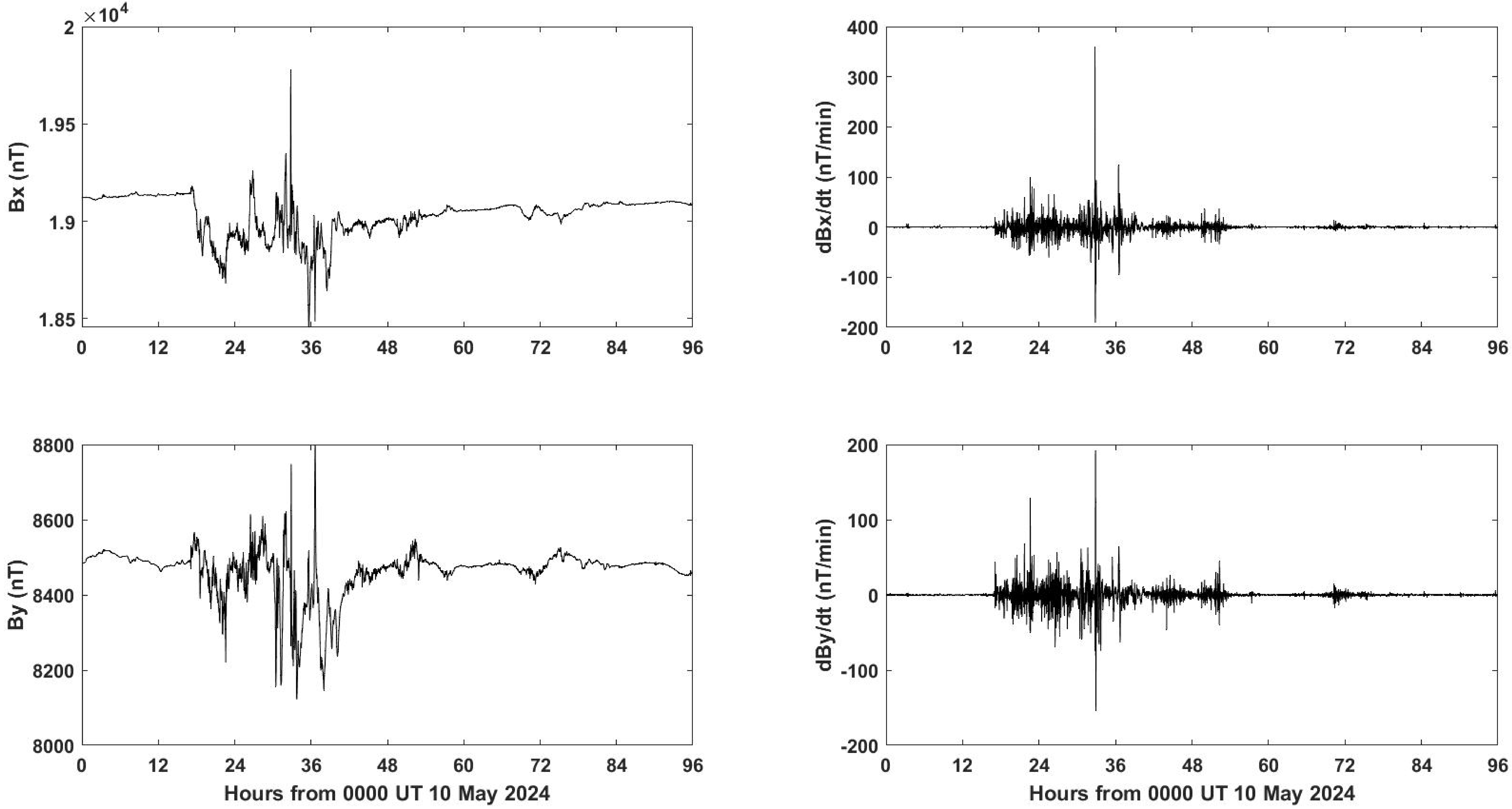
×10^4
2
1.95
Bx (nT)
1.9
1.85
0 12 24 36 48 60 72 84 96
400
300
200
dBx/dt (nT/min)
100
0
-100
-200
0 12 24 36 48 60 72 84 96
8800
8600
By (nT)
8400
8200
8000
0 12 24 36 48 60 72 84 96
Hours from 0000 UT 10 May 2024
200
100
dBy/dt (nT/min)
0
-100
-200
0 12 24 36 48 60 72 84 96
Hours from 0000 UT 10 May 2024

Figure 4.

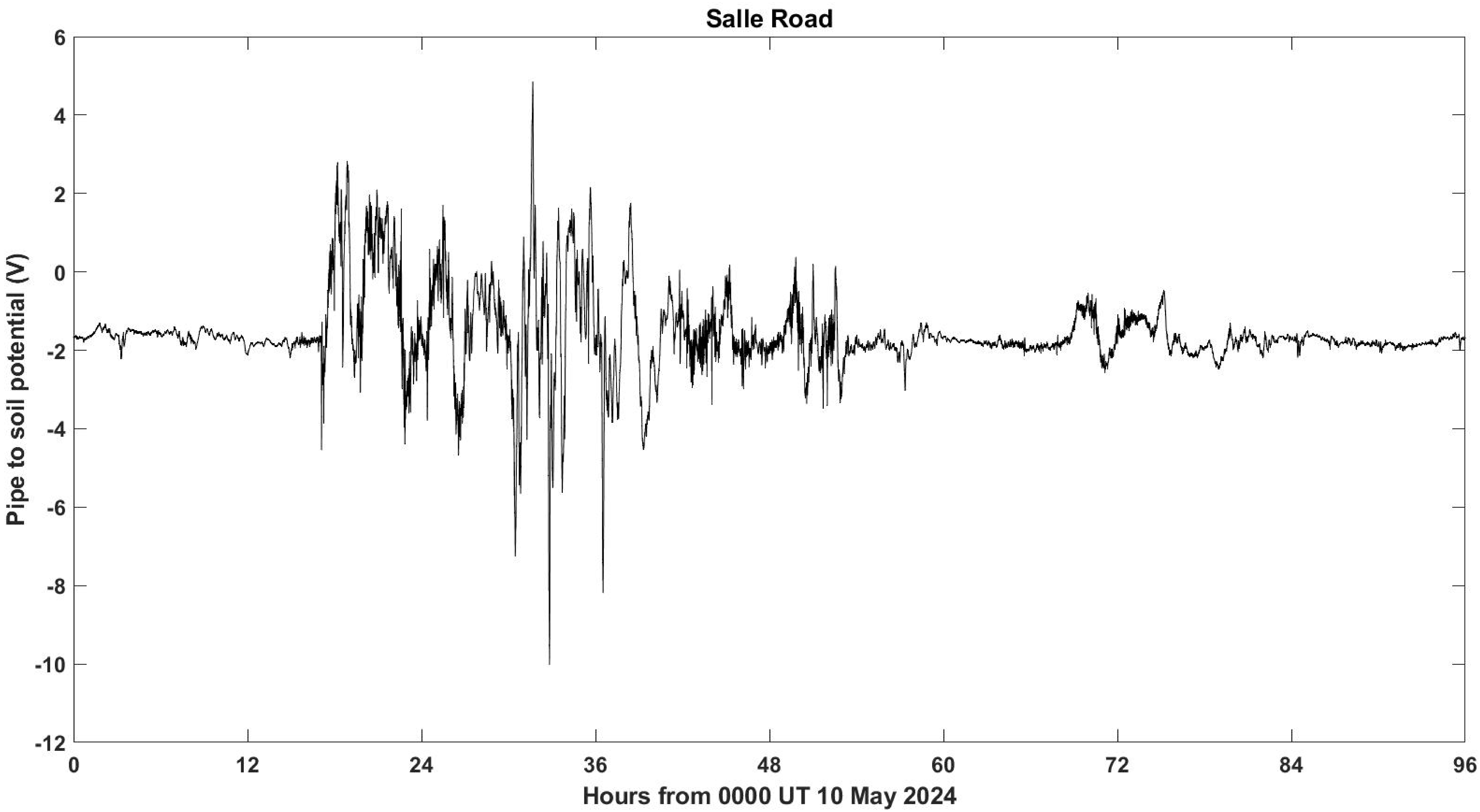

Salle Road
Pipe to soil potential (V)
6
4
2
0
-2
-4
-6
-8
-10
-12
0
12
24
36
48
60
72
84
96
Hours from 0000 UT 10 May 2024

Figure 5.

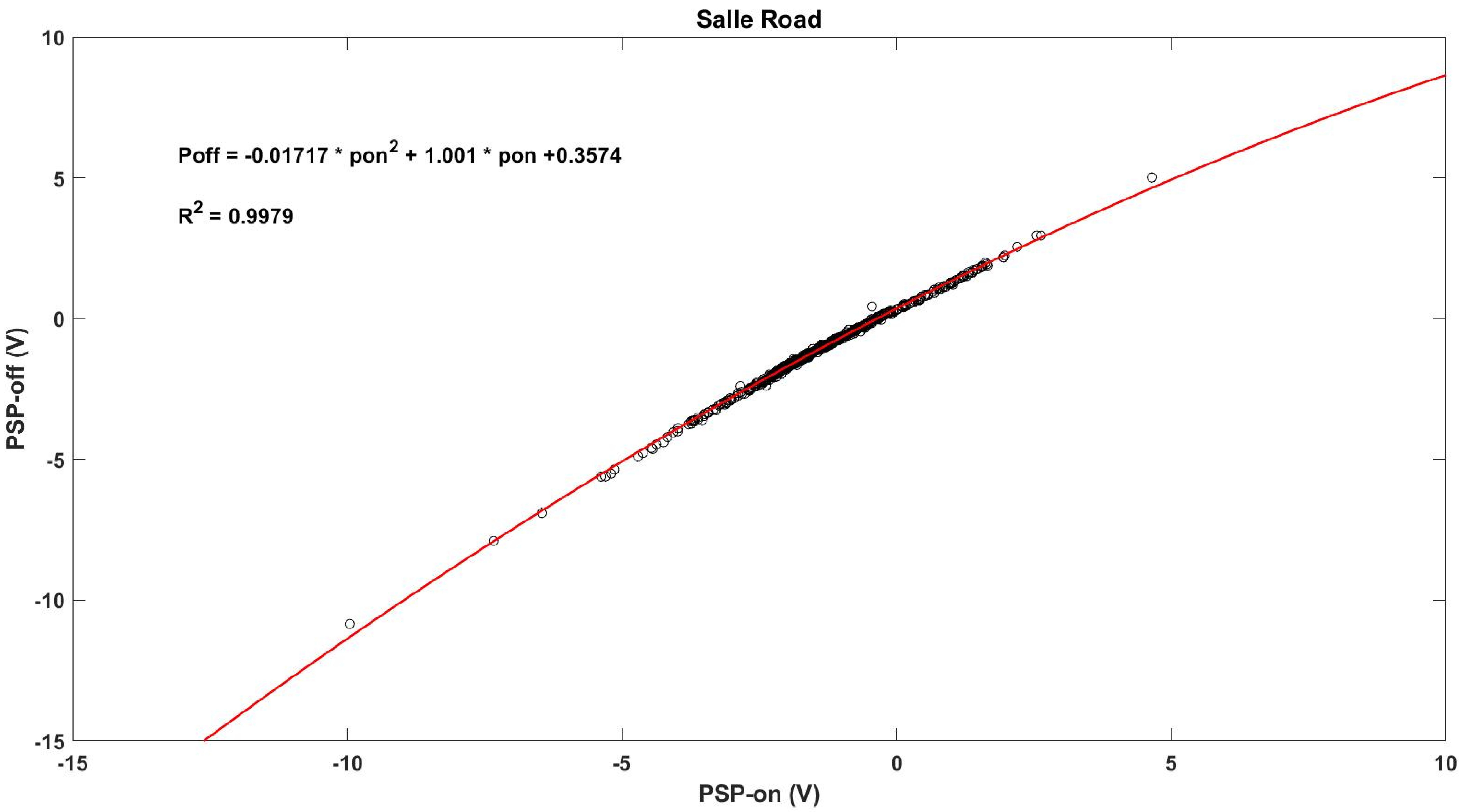
Salle Road
Poff = -0.01717 * pon^2 + 1.001 * pon +0.3574
R^2 = 0.9979
PSP-off (V)
PSP-on (V)
10
5
0
-5
-10
-15
-15
-10
-5
0
5
10

Figure 6.

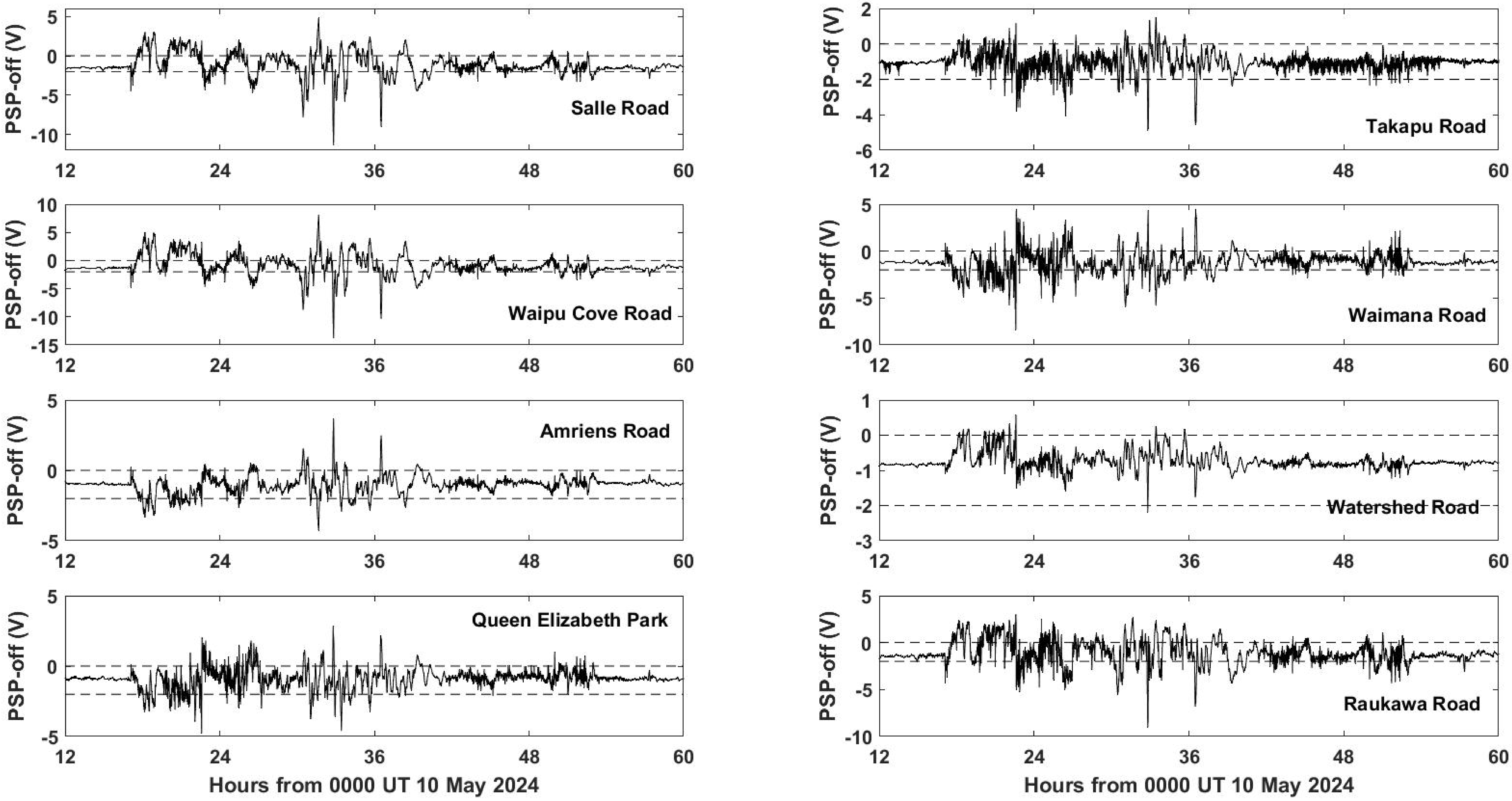
PSP-off (V)
Salle Road
Waipu Cove Road
Amriens Road
Queen Elizabeth Park
Takapu Road
Waimana Road
Watershed Road
Raukawa Road
Hours from 0000 UT 10 May 2024

Figure 7.

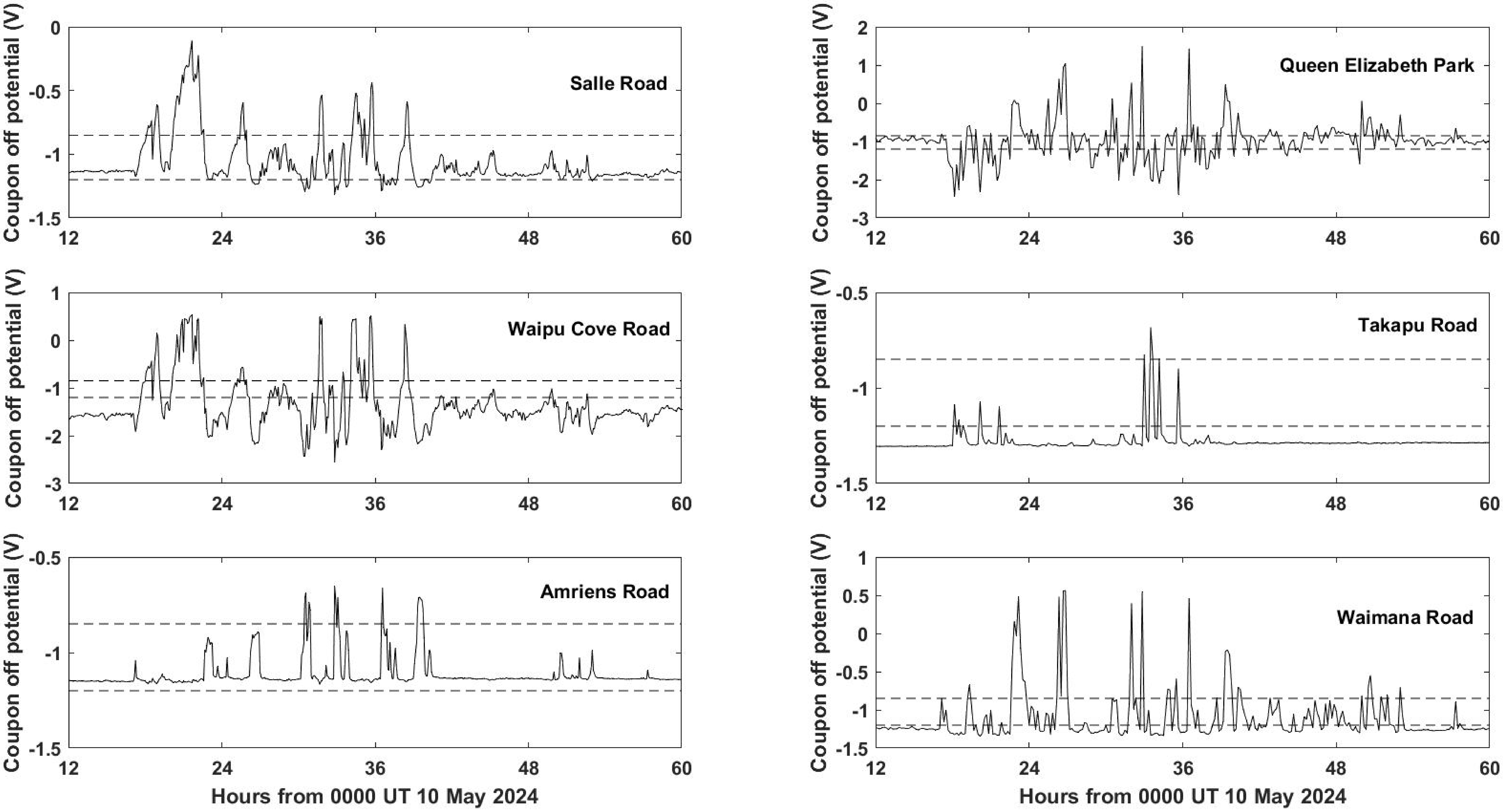
Salle Road
Waipu Cove Road
Amriens Road
Queen Elizabeth Park
Takapu Road
Waimana Road
Coupon off potential (V)
Hours from 0000 UT 10 May 2024
12
24
36
48
60

Figure 8.

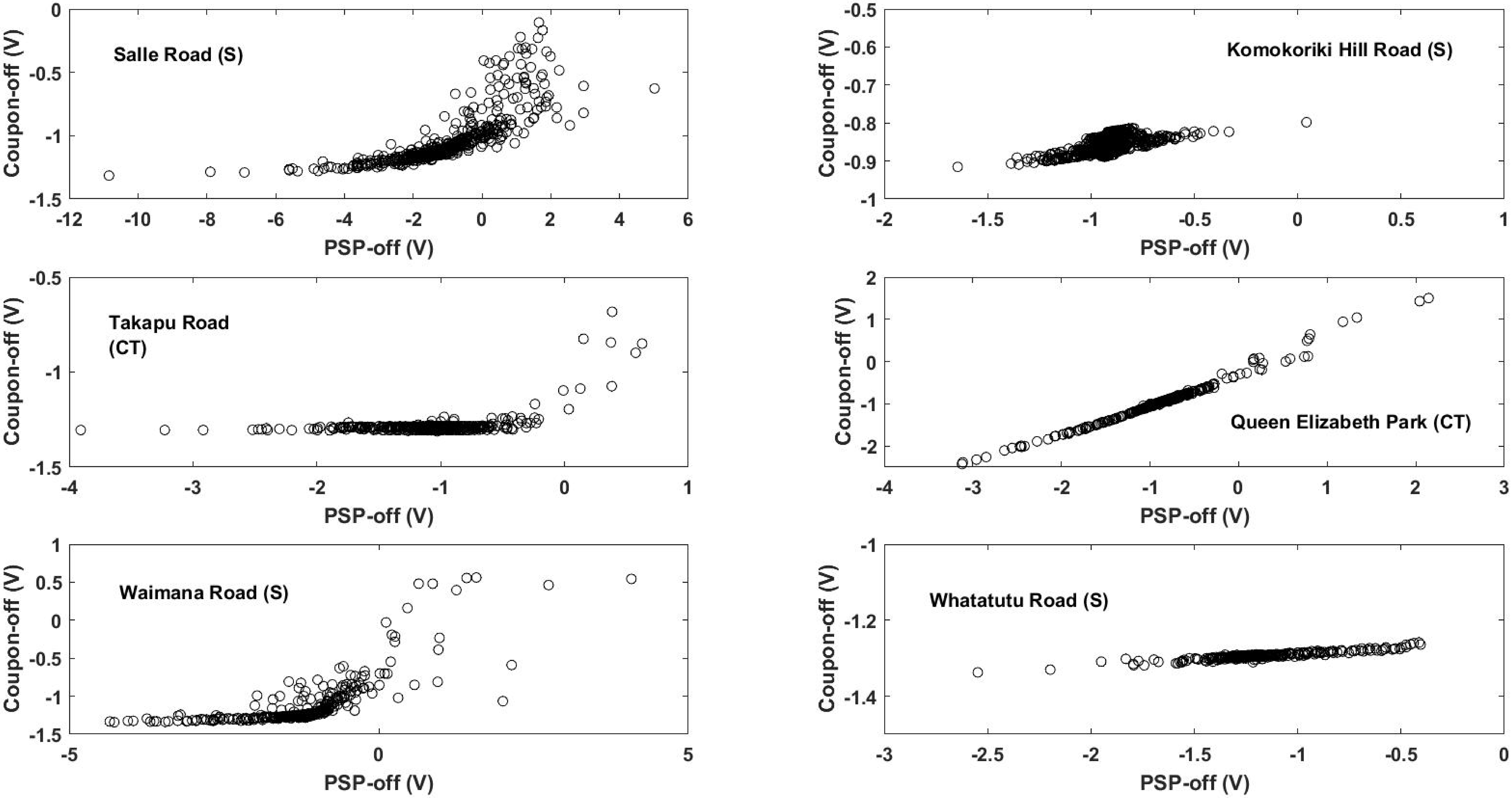
Salle Road (S)
Komokoriki Hill Road (S)
Takapu Road (CT)
Queen Elizabeth Park (CT)
Waimana Road (S)
Whatatutu Road (S)
Coupon-off (V)
PSP-off (V)

Figure 9.

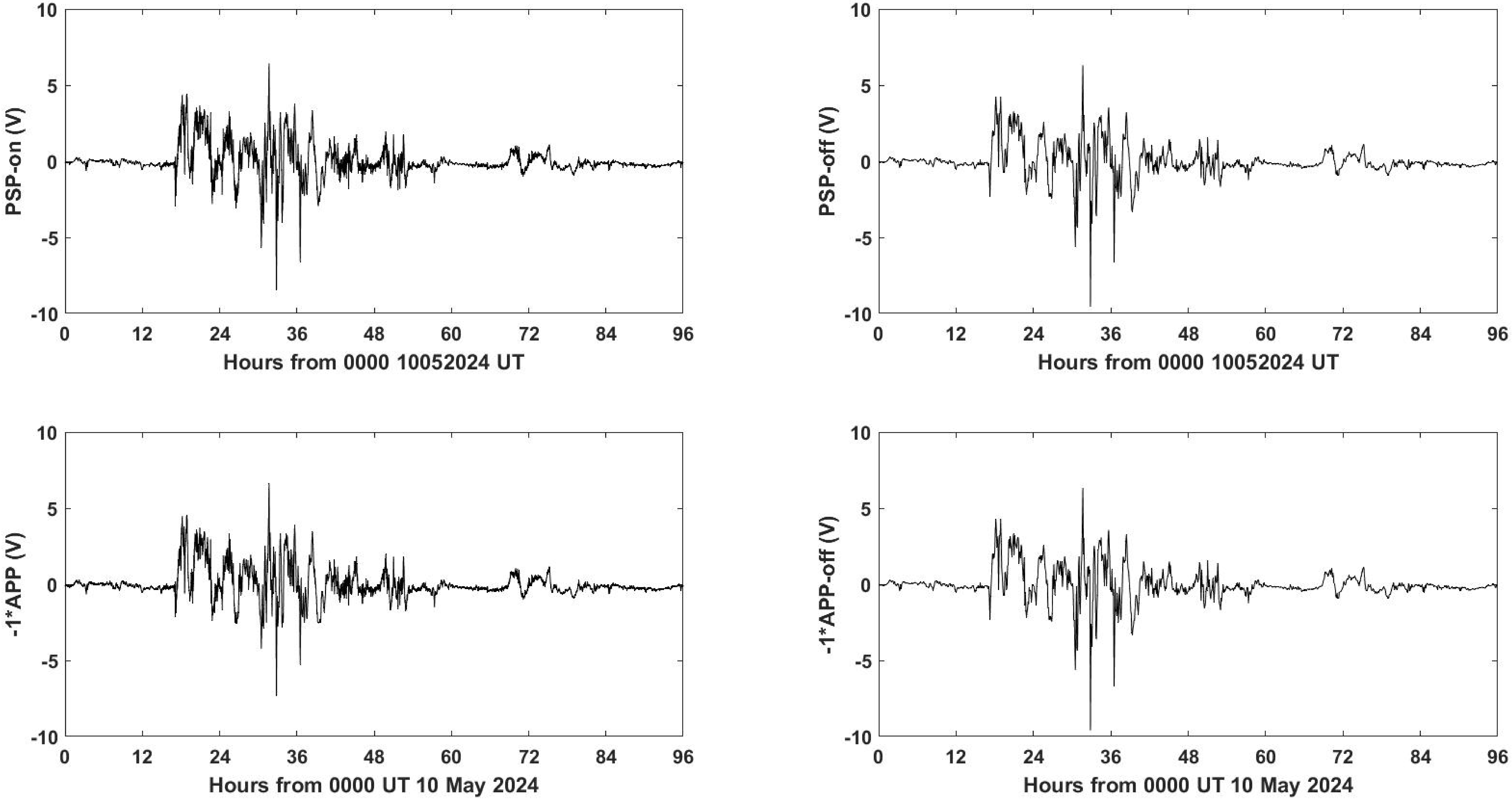
PSP-on (V)
Hours from 0000 10052024 UT
PSP-off (V)
Hours from 0000 10052024 UT
-1*APP (V)
Hours from 0000 UT 10 May 2024
-1*APP-off (V)
Hours from 0000 UT 10 May 2024

Figure 10.

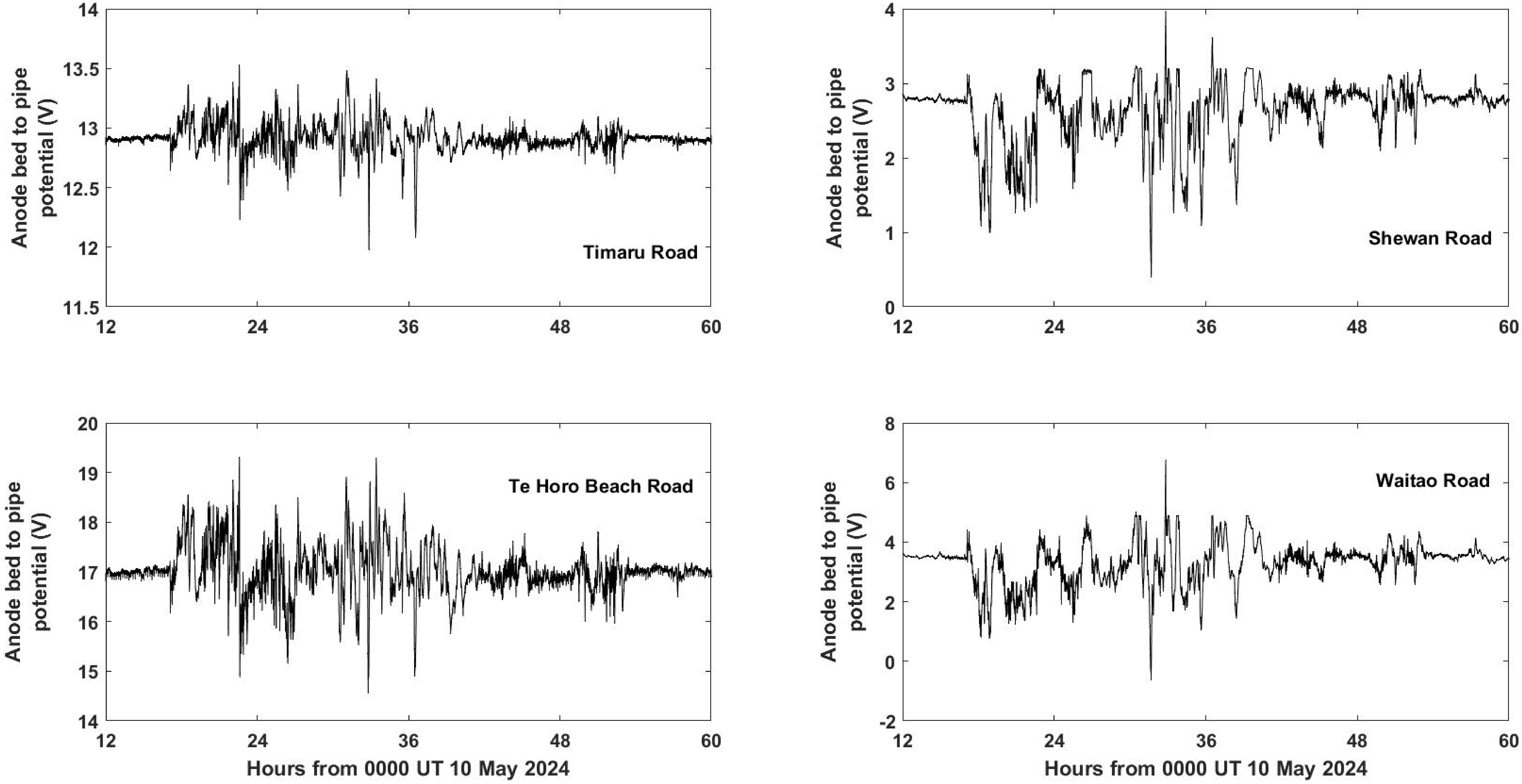
Timaru Road
Shewan Road
Te Horo Beach Road
Waitao Road
Anode bed to pipe potential (V)
Hours from 0000 UT 10 May 2024
14
13.5
13
12.5
12
11.5
4
3
2
1
0
20
19
18
17
16
15
14
8
6
4
2
0
-2
12
24
36
48
60

Figure 11.

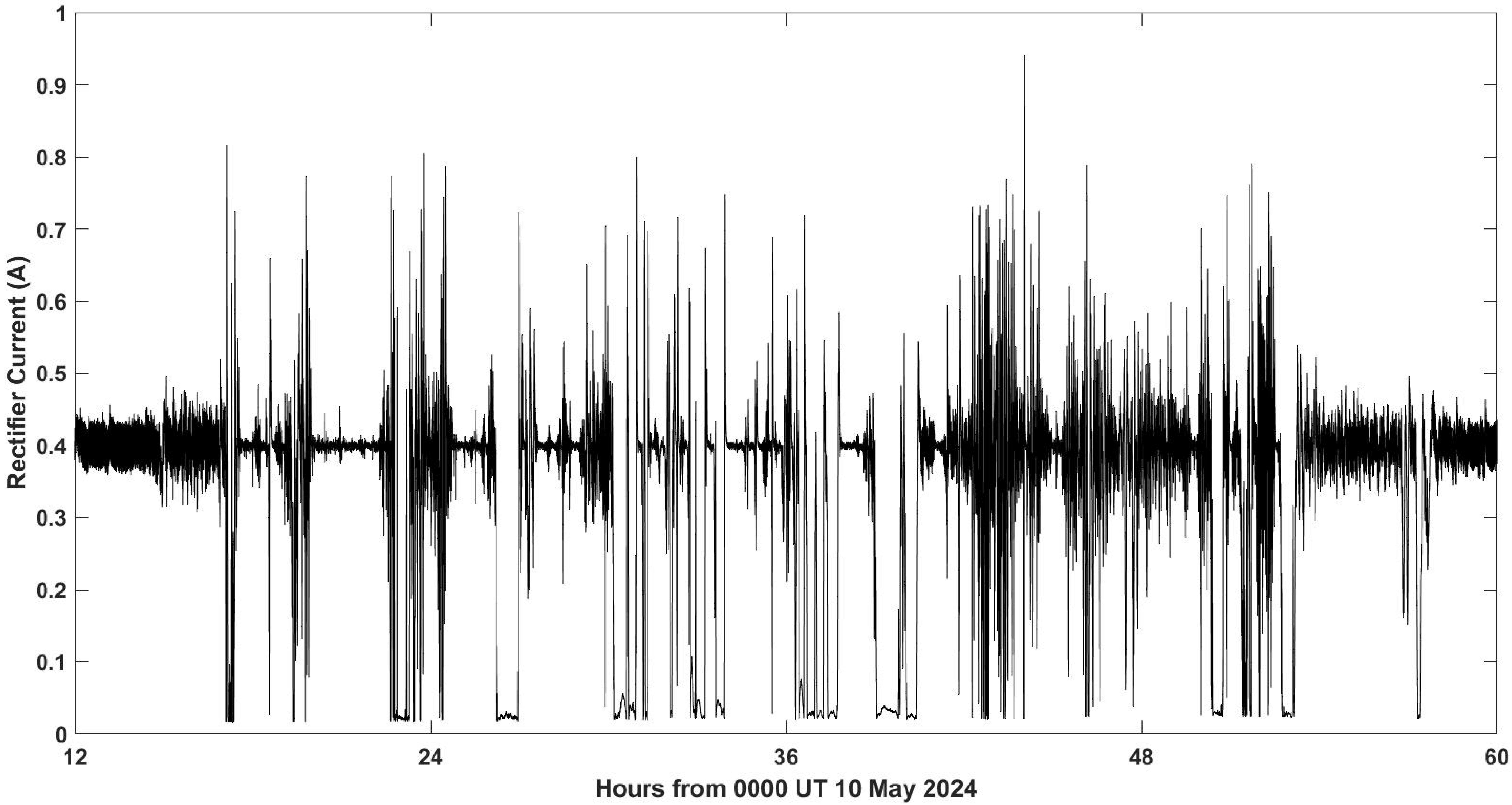

Rectifier Current (A)
0
0.1
0.2
0.3
0.4
0.5
0.6
0.7
0.8
0.9
1
12
24
36
48
60
Hours from 0000 UT 10 May 2024

Figure 12.

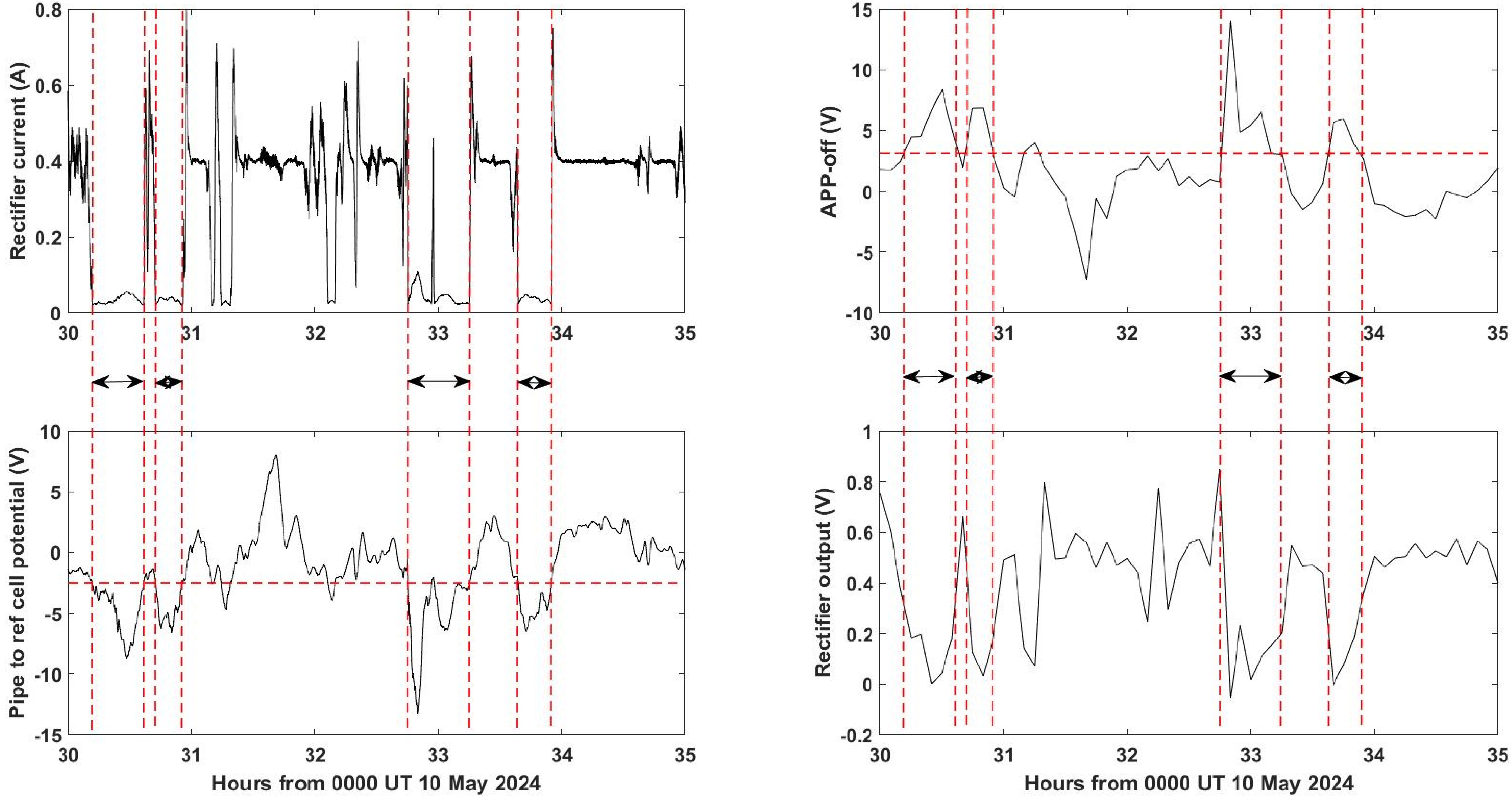
Rectifier current (A)
APP-off (V)
Pipe to ref cell potential (V)
Rectifier output (V)
Hours from 0000 UT 10 May 2024
Hours from 0000 UT 10 May 2024